Bull Mater Sci (2021) 44:43
https://doi.org/10.1007/s12034-020-02316-y

Push-pull effect on the charge transport characteristics in V-shaped organic semiconductor materials

AHMAD IRFAN[1,2]
[1]Research Center for Advanced Materials Science, King Khalid University, Abha 61413, Saudi Arabia
[2]Department of Chemistry, Faculty of Science, King Khalid University, Abha 61413, Saudi Arabia
irfaahmad@gmail.com

MS received 26 June 2020; accepted 16 October 2020

Abstract. With the goal to tune charge transport and electronic properties of 4,6-di(thiophen-2-yl)pyrimidine (DTP) structure, seven novel V-shaped organic semiconductor compounds were designed by nitrogen doping, oligocenes π-bridge incorporations and push-pull strategy. Primarily, 4,6-bis-thiazol-2-yl-pyrimidine (**1**) was designed by nitrogen atoms doping in DTP. Then push-pull system named **1DA** was designed by substituting $-N(CH_3)_2$ at R_1 and R_2, while $-CF_3$ at R_3 and R_4 positions of **1**. Moreover, various semiconducting materials (**2DA-6DA**) with tuned properties were designed from **1DA** by fusing benzene, naphthalene, anthracene, tetracene and pentacene at both ends. The density functional theory (DFT) and time-dependent DFT were adopted for optimizing the ground and excited state structures, correspondingly. We investigated frontier molecular orbitals, photo-stability, electron injection, electron affinity (EA), ionization energies (IE) and reorganization energies. The push-pull and π-bridge elongation strategies ominously raise EA while diminish IE values, which may lead to decrease the electron and hole injection obstruction. Besides, donors–acceptors and oligocenes at both ends meaningfully drop the electron reorganization energy values as compared to normally used *n*-type material, i.e., tris(8-hydroxyquinolinato)aluminium (*mer*-Alq3). These results revealed that newly designed materials **4DA-6DA** would be proficient to be used in *n*-type semiconductor devices.

Keywords. Organic semiconductors; oligocenes; tris(8-hydroxyquinolinato)aluminium; charge transport; electronic properties.

1. Introduction

The organic materials (OMs) are being used in various semiconductor devices because of the good charge mobility and tunable properties. These OMs have multidisciplinary applications in semiconductor devices as energy conversion, optoelectronic along with photovoltaics [1]. Recently, OMs have developed several devices within OLEDs along with organic field-effect transistors (OFETs) [2–4]. The OMs are focus of study for synthetic experts as well as theoreticians [5] because of the multi-purpose applications [6,7]. The thiophene-based materials have also interesting applications in optoelectronic devices. The latest works on conjugated acenes and hydrocarbons have widened its application in electronics industry promptly [8–11]. It is the dire need to synthesize acene substituents with better mobility and stability.

Presently, quantum chemical approaches are being carried out to unveil various properties of interests. Various structural modifications are well-thought-out as unsurpassed tactic to tune optoelectronic and charge transport properties of organic semiconductor materials (OSMs). The energy of lowest unoccupied molecular orbital (E_{LUMO}), energy of highest occupied molecular orbital (E_{HOMO}), electron affinity (EA), ionization energies (IE) and reorganization energy (λ) were explored to analyse OSMs characteristics [12].

Density functional methods attained progress and these are ascribed first-rate predictive power for the calculation of charge transport and electro-optical properties. The density functional theory (DFT) [13–15] calculations usually facilitates the molecular system elucidation with esteem to electronic properties. The intra-molecular charge transfer (ICT) is used to enhance the rate of charge transfer, reducing the structural deviation along with polarization after electron-deficient group's incorporation [16]. The eco-friendly and cost-effective organic compounds are ease to prepare [17]. Furthermore, OMs with chain elongation skilled pleasing charge transport and electro-optical characteristics. The improved electronic applications of these OMs after auspicious chain conformation [18–20] are

Electronic supplementary material: The online version of this article (https://doi.org/10.1007/s12034-020-02316-y) contains supplementary material, which is available to authorized users.

Published online: 18 February 2021

tremendously prolific with suitable E_{HOMO}, E_{LUMO}, IE as well as EA [21]. For the fabrication of proficient OSMs, acenes were deliberated as decidedly encouraging compounds [22,23]. For the management of charge transport and electro-optical characteristics of these OMs, the π-conjugated cores, end groups and substitution of heteroatoms are promising approach [7]. Moreover, to augment the charge transport characteristics, introduction of numerous π-conjugated bridges within designed compounds would be a nice approach [24,25].

Hitherto, 4,6-di(thiophen-2-yl)pyrimidine (DTP) was found as an admirable building block to design competent optoelectronic materials [26]. In order to further tune charge transport as well as electronic characteristics, seven novel V-shaped organic semiconductor systems were designed by nitrogen doping, oligocenes π-bridge elongation and push-pull strategy. Firstly, nitrogen atoms were doped in DTP to get 4,6-bis-thiazol-2-yl-pyrimidine (**1**). Then $–N(CH_3)_2$ at R_1/R_2 while $–CF_3$ at R_3/R_4 positions of **1** were introduced to get push-pull system, named **1DA**. Additionally, few more push-pull semiconducting systems (**2DA-6DA**) were designed from **1DA** by elongating both ends with benzene, naphthalene, anthracene, tetracene and pentacene incorporation, as shown within figure 1. The article is well prepared regarding new methodology as prescribed within section 2 in detail. Furthermore, in section 3 the electronic properties, distribution pattern of the frontier molecular orbitals and energies of HOMO and LUMO, and charge transport characteristics (vertical/adiabatic EA, vertical/adiabatic IE and hole/electron λ) are discussed.

2. Methodology

The benchmark study was executed to probe the electronic properties. The S_0 geometry of DTP was computed at B3LYP, LC-BLYP, M05 and M05-2X functionals along with 6-31G** basis set. It was found that LC-BLYP, M05 and M05-2X functionals overestimate the energy gaps (E_{gap}), while B3LYP rationally reproduce experimental data [26]. The standard DFT functional (B3LYP) established the best explanation regarding geometry alterations upon ionization [27] in ground state (S_0) optimization [24,28,29]. Currently, 6-31G** basis set [30] level using B3LYP [31] functional were used for computational purposes. The TDDFT have been used for the λ_{abs} calculation proved it as an efficient methodology [32]. The charge transport capability performs central function within various organic layer(s). The recombination processes in the bulk supported with their higher-charge mobility's, in which charges could be limited through organic–organic interfaces [33]. Marcus theory was used for the measurement of rate of charge transfer as per equation (1) [34].

$$W = V^2/h(\pi/\lambda k_B T)^{1/2}\exp(-\lambda/4k_B T) \quad (1)$$

The rates of self-exchange electron-transfer along with their charge mobility used to calculate with two major standards are: (i) λ, which should be small for significant transport, along with (ii) neighbouring compounds transfer integral (V) or electronic coupling that should be optimized. The term λ characterizes the intensity regarding electron–phonon interactions (vibration) and it was evaluated doubled compared with polaron localized relaxation energy considering individual entity. The λ unit may be segregated within two components: $\lambda_{rel}^{(1)}$ and $\lambda_{rel}^{(2)}$. The relaxation energy geometry for one compound from neutral to charged state resembles with $\lambda_{rel}^{(1)}$ and relaxation energy geometry from same compound from charged to neutral state corresponds to $\lambda_{rel}^{(2)}$ [35].

$$\lambda = \lambda_{rel}^{(1)} + \lambda_{rel}^{(2)} \quad (2)$$

For λ, the two other terms were calculated with the help of adiabatic potential energy surfaces directly. The assessment of two components of λ were determined quickly in accordance with adiabatic potential energy surfaces with the help of equation (3) [36].

$$\lambda = \lambda_{rel}^{(1)} + \lambda_{rel}^{(2)} = \left[E^{(1)}(L^+) - E^{(0)}(L^+)\right] + \left[E^{(1)}(L) - E^{(0)}(L)\right] \quad (3)$$

In the above equation (3), the term $E^{(0)}(L)$ and $E^{(0)}(L^+)$ represent neutral ground-state energies (optimized) along with charged ones. The $E^{(1)}(L)$ is neutral compound energy with optimized charged geometry, whereas $E^{(1)}(L^+)$ is the energy of the charged state with geometry of the optimized neutral compound. It is important to observe that surrounding compounds polarization impact along with realignment of their charges were ignored in order to reduce the theoretical computations complications [37]. By using theory of B3LYP/6-31G** level, the values of adiabatic/vertical EA ($EA_{a/v}$) and adiabatic/vertical IE ($IE_{a/v}$) were calculated. All computations were performed with the help of Gaussian 16 software package [38].

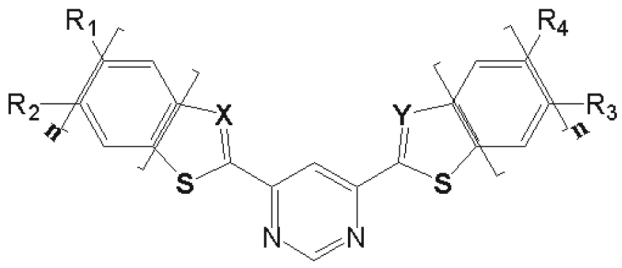

DTP; R_1, R_2, R_3, R_4 = H and X, Y = C while n = 0
1; R_1, R_2, R_3, R_4 = H and X, Y = N while n = 0
1DA; R_1, R_2 = -$N(CH_3)_2$; R_3, R_4 = -CF_3 and X, Y = N while n = 0
2DA; R_1, R_2 = -$N(CH_3)_2$; R_3, R_4 = -CF_3 and X, Y = N while n = 1
3DA; R_1, R_2 = -$N(CH_3)_2$; R_3, R_4 = -CF_3 and X, Y = N while n = 2
4DA; R_1, R_2 = -$N(CH_3)_2$; R_3, R_4 = -CF_3 and X, Y = N while n = 3
5DA; R_1, R_2 = -$N(CH_3)_2$; R_3, R_4 = -CF_3 and X, Y = N while n = 4
6DA; R_1, R_2 = -$N(CH_3)_2$; R_3, R_4 = -CF_3 and X, Y = N while n = 5

Figure 1. The structures of DTP and derivatives examined in this study.

3. Results and discussion

3.1 *Electronic properties*

The computed values of energies of the frontier molecular orbitals, i.e., HOMO/LUMO energies (E_{HOMO}/E_{LUMO}) and their energy gaps (E_{gap}) are displayed in table 1. The estimated values of E_{HOMO}/E_{LUMO} of DTP were –6.19/–1.94 at ground state (S_0), respectively [39]. The computed E_{HOMO}/E_{LUMO} of designed derivatives **1** as well as **1DA-6DA** are –6.60/–2.35, –5.22/–2.57, –5.42/–2.72, –5.35/–2.81, –4.96/–2.90, –4.68/–3.02 and –4.47/–3.12 at S_0, respectively. One can see that nitrogen atoms doping at –X and –Y places (**1**) lowers the E_{HOMO} and E_{LUMO} levels than DTP. The substitution of $–N(CH_3)_2$ at R_1/R_2 while $–CF_3$ at R_3/R_4 positions in **1** higher the E_{HOMO}, while lowers the E_{LUMO} levels. It was also found that benzene, naphthalene, anthracene, tetracene and pentacene incorporation at both ends of **1DA** significantly lowers the E_{LUMO} levels of **2DA-6DA**. Moreover, anthracene, tetracene and pentacene incorporation at both ends of **1DA** expressively lowers the E_{HOMO} levels of **4DA-6DA**. This strategy of integration would be helpful for designing *p*- as well as *n*-type efficient materials. The trend in the E_{gaps} was found as DTP (4.25) = **1** (4.25) > **2DA** (2.70) > **1DA** (2.65) > **3DA** (2.54) > **4DA** (2.06) > **5DA** (1.67) > **6DA** (1.35) eV. The E_{gap} is significantly decreased after incorporation of pentacene at both ends along with donors and acceptors from 4.25 to 1.35. The assessed values of E_{HOMO}/E_{LUMO} of DTP were –6.02/–2.10 at excited state (S_1), respectively. The computed E_{HOMO}/E_{LUMO} of designed derivatives **1** as well as **1DA-6DA** are –6.23/–2.68, –4.70/–2.82, –4.94/–2.86, –5.17/–2.88, –4.63/–2.95, –4.68/–3.23 and –4.32/–3.12 at S_1, respectively. The nitrogen doping at –X and –Y places (**1**) lowers the E_{HOMO} and E_{LUMO} levels than parent compound. The substitution of $–N(CH_3)_2$ at R_1/R_2 while $–CF_3$ at R_3/R_4 positions in **1** higher the E_{HOMO}, while lowers the E_{LUMO} levels. It was also found that oligocene moieties fusion at both ends of **1DA** considerably lowers the E_{LUMO} levels of **2DA-6DA** than that of prior one. Likewise, anthracene, tetracene and pentacene incorporation at both ends of **1DA** expressively lowers the E_{HOMO} levels of **4DA-6DA**. The trend in the E_{gaps} was found as DTP (3.92) = **1** (3.55) > **3DA** (2.29) > **2DA** (2.08) > **1DA** (1.88) > **4DA** (1.68) > **5DA** (1.45) > **6DA** (1.20) eV. The nitrogen doping in parent compound significantly lowers the LUMO energy level as compared to DTP, see table 4. In this study, the effect of donor and acceptor has also been explored. The nitrogen doping along with EDGs and EWDGs substitutions also considerably higher the HOMO levels, while lower the LUMO energy levels resulting to reduce the energy gap of newly designed derivatives as compared to **DTP1-DTP3**, for details see supplementary figure S1 and table S1. It is foreseen that this tactic of oligocene integration and push-pull strategy would be supportive for designing longer wavelength and proficient semiconductor materials. HOMOs and LUMOs formation patterns for studied compounds at S_0 and S_1 are presented within figures 2 and 3. The formation of HOMO charge has been delocalized on donor side while LUMO localized on central electron-deficient ring and/or acceptor side. In all studied molecules, the ICT was perceived from occupied to unoccupied molecular orbitals.

The work functions (*W*) with regard to Au and Al electrodes are 5.10 and 4.08 eV, respectively [40]. From this, we inspected hole/electron injection energies (HIE/EIE) of DTP derivatives (**1** and **1DA-6DA**) with respect to Au and Al electrodes individually as (EIE = $-E_{LUMO}$ − (−*W* of metal)) and (HIE = − *W* of metal − ($-E_{HOMO}$)). The results of theoretical EIE revealed that **2DA-6DA** could show more assistance for hole and electron injection when compared with DTP and **1**. Moreover, it can be perceived that Al may be appropriate electrode for its better ability towards

Table 1. Ground and excited states energies (E_{HOMO} and E_{LUMO}), and their energy gaps (E_{gap})[a] in eV at the B3LYP/6-31G** and TD-B3LYP/6-31G** levels, respectively.

Complexes	Ground state			First excited state		
	E_{HOMO}	E_{LUMO}	E_{gap}	E_{HOMO}	E_{LUMO}	E_{gap}
DTP	–6.19	–1.94	4.25	–6.02	–2.10	3.92
	(–9.05)[b]	(0.35)[b]	(9.40)[b]			
	(–6.51)[c]	(–1.71)[c]	(4.80)[c]			
	(–7.60)[d]	(–1.00)[d]	(6.60)[d]			
1	–6.60	–2.35	4.25	–6.23	–2.68	3.55
1DA	–5.22	–2.57	2.65	–4.70	–2.82	1.88
2DA	–5.42	–2.72	2.70	–4.94	–2.86	2.08
3DA	–5.35	–2.81	2.54	–5.17	–2.88	2.29
4DA	–4.96	–2.90	2.06	–4.63	–2.95	1.68
5DA	–4.68	–3.01	1.67	–4.68	–3.23	1.45
6DA	–4.47	–3.12	1.35	–4.32	–3.12	1.20

[a]Experimental E_{HOMO}, E_{LUMO} and E_{gap} are –5.30, –1.90 and 3.40 eV, respectively from [26].
[b,c,d]E_{HOMO}, E_{LUMO} and E_{gap} at LC-BLYP/6-31G**, M05/6-31G** and M052X/6-31G** levels, respectively.

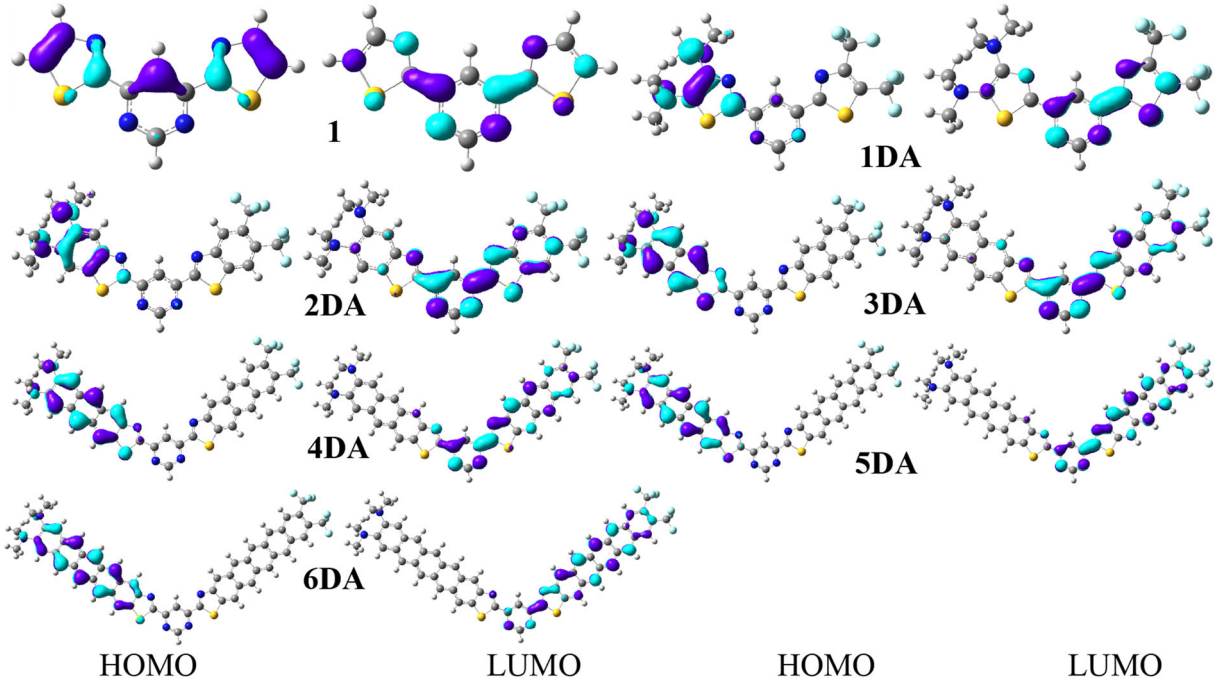

Figure 2. Distribution pattern of the frontier molecular orbitals of studied compounds at ground states.

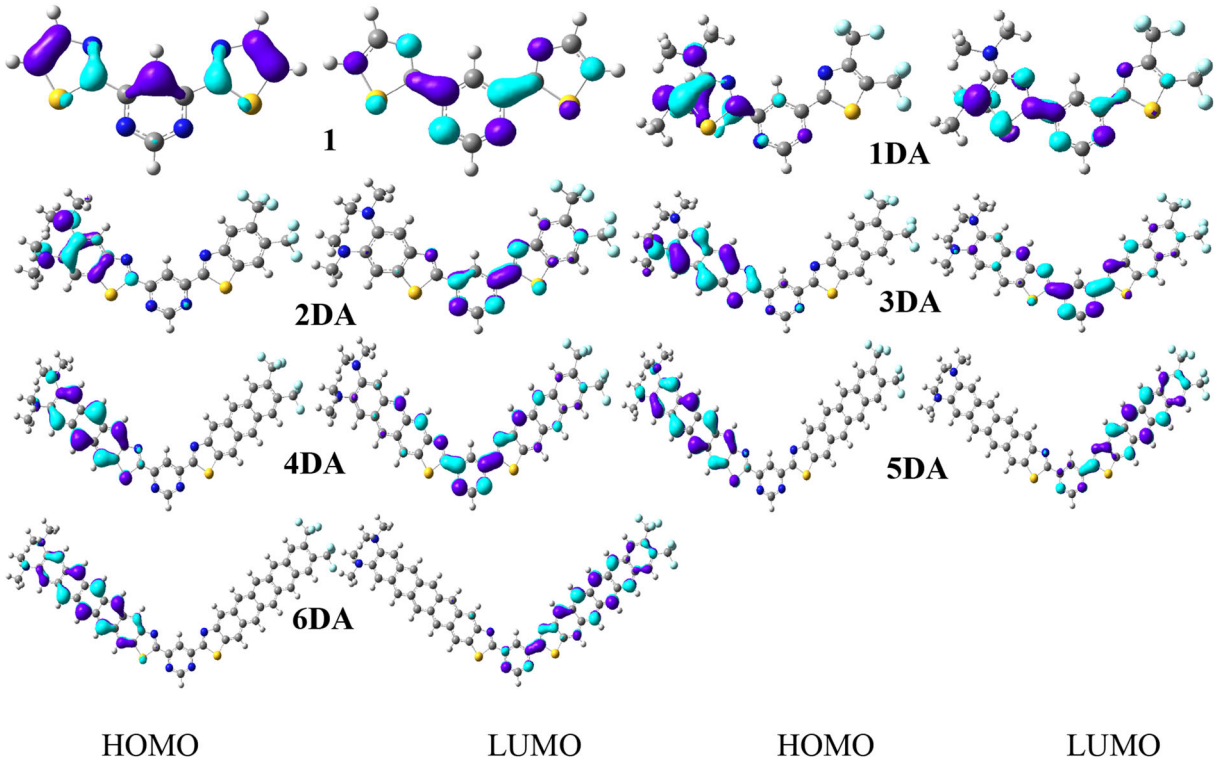

Figure 3. Distribution pattern of the HOMOs and LUMOs of studied compounds at excited states.

electron and hole injection, except for **2DA-4DA** in which Au might be better for hole injection, see table 2. When Al electrode was used, the EIE and HIE energy hurdles are suggestively declined after oligocene groups incorporation. It can be also seen that nitrogen doping in DTP decreased the electron injection barrier while increase the hole injection barrier as in compound **1**. Furthermore, the substitution of donors and acceptors decrease hole injection barrier while increase the electron one as in **1DA** compared to **1**. From the results, it is predicted that this method would be

Table 2. Electron injection energy (EIE) and hole injection energy (HIE) barriers of DTP derivatives calculated at B3LYP/6-31G** level.

Parameters	DTP	**1**	**1DA**	**2DA**	**3DA**	**4DA**	**5DA**	**6DA**
HIE (Au)	1.09	1.50	1.09	0.12	0.32	0.25	−0.14	−0.42
EIE (Au)	3.16	2.75	3.16	2.53	2.38	2.29	2.2	2.09
HIE (Al)	2.11	2.52	2.11	1.14	1.34	1.27	0.88	0.60
EIE (Al)	2.14	1.73	2.14	1.51	1.36	1.27	1.18	1.07

Table 3. η, μ, S, χ and ω in eV of DTP and derivatives at B3LYP/6-31G** level.

Parameters	DTP	**1**	**1DA**	**2DA**	**3DA**	**4DA**	**5DA**	**6DA**
Hardness (η)	3.62	3.65	2.76	2.68	2.48	2.12	1.83	1.60
Potential (μ)	−4.06	−4.46	−3.93	−4.13	−4.14	−3.99	−3.89	−3.83
Softness (S)	1.05	1.11	1.21	1.27	1.33	1.44	1.56	1.69
Electronegativity (χ)	4.06	3.46	3.93	4.13	4.14	3.99	3.89	3.83
Electrophilic index (ω)	2.27	2.73	2.80	3.18	3.45	3.75	4.13	4.58

supportive for designing improved hole and electron injection materials for semiconductor substances.

The essential parameters like global chemical reactivity descriptors (GCRD) are used to figure out the reactivity and structure stability. Currently we have computed GCRD theoretical parameters as for example, softness (S), electronegativity (χ), chemical potential (μ), chemical hardness (η) along with electrophilicity index (ω) values for DTP-derived products with the help of IE and EA, see table 3.

Hence, the hardness of any materials corresponds to the gap between the HOMO and LUMO orbitals. If the energy gap of HOMO–LUMO is larger, then molecule would be harder [41].

$$\eta = \frac{1}{2}(\mathrm{EA} - \mathrm{EA}) \tag{4}$$

The electronic chemical potential (μ) of a molecule is calculated by:

$$\mu = -\left(\frac{\mathrm{IE} + \mathrm{EA}}{2}\right) \tag{5}$$

The softness of a molecule is calculated by:

$$S = \frac{I}{2\eta} \tag{6}$$

The electronegativity of the molecule is calculated by:

$$\chi = \left(\frac{\mathrm{IE} + \mathrm{EA}}{2}\right) \tag{7}$$

The electrophilicity index of the molecule is calculated by:

$$\omega = \frac{\mu^2}{2\eta} \tag{8}$$

The calculated values of GCRD, such as η, μ, S, χ and ω for studied molecules are also presented in table 3.

The η of molecule is interrelated to aromaticity [42,43]. The μ expresses the electron tendency to get await from its electronic cloud environment. The η value represents the degree of impediment of the electronic cloud distortion and stabilization energy values denote with ω. The obtained values of μ demonstrated the donor and acceptor groups along with oligocenes, within parent compound uncovered the tendency to provide particles in newly designed derivatives (**1DA-6DA**), would be smaller which would enhance the stability of these compounds. Moreover, smaller η values of the designed compounds (**4DA-6DA**) are revealing that these derivatives would be more stable.

3.2 *Molecular electrostatic potential*

The molecular electrostatic potential (MEP) is appropriate parameter to examine the reactivity of different molecules and/or species. Actually, MEP is a noticeable property that could be experimentally evaluated through diffraction spectrum [44,45]. Furthermore, it might be explored through computational resources. It also demonstrates the broad range nuclear and electronic charge allocation that is an applicable aspect to figure out different species interactions. The colour displays in figure 4 showed the MEP mapped surfaces. Within MEP, the higher negative potential zones, indicated through red colour spot, are helpful in order to electrophilic substitution, while higher positive potential zones, shown with blue colour spot, classify favourable towards nucleophilic substitution attack. The positive MEP reduces according to the following colour

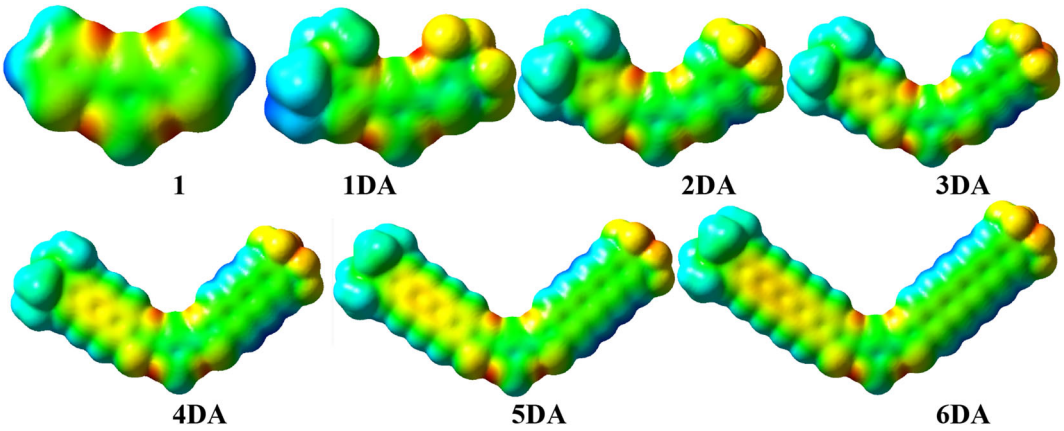

Figure 4. MEP of studied compounds.

Table 4. Ionization energies (IE), electronic affinities (EA), reorganization energies (λ(h) and λ(e)) (in eV) at the B3LYP/6-31G** level.

Complexes	IE_a	EA_a	IE_v	EA_v	λ(h)	λ(e)
DTP	7.58	0.54	7.68	0.43	0.202	0.228
1	8.00	0.95	8.12	0.81	0.239	0.293
1DA	6.26	1.42	6.70	1.17	0.877	0.501
2DA	6.45	1.64	6.81	1.45	0.725	0.378
3DA	6.44	1.82	6.62	1.66	0.486	0.312
4DA	6.02	1.98	6.11	1.87	0.194	0.233
5DA	5.65	2.14	5.73	2.06	0.160	0.171
6DA	5.38	2.30	5.44	2.23	0.134	0.133

ordering blue > green > yellow > orange > red. The greater repulsion were observed in red colour areas, whereas blue colour area explained the adequate attraction for nucleophilic attack and vice versa.

The negative electrostatic potential was found on the –N atoms and acceptor groups ($-CF_3$), while positive one at hydrogen atoms and donor moieties ($-N(CH_3)_2$). It is foreseen that considerable repulsion might be at –N atoms and $-CF_3$ along with significant attraction towards hydrogen atoms and $-N(CH_3)_2$ groups, wherein nucleophilic attack occur. Although in the case electrophilic substitution occur, momentous repulsion could occur towards –H atoms and $-N(CH_3)_2$ groups along with prominent attraction would be at –N atoms and $-CF_3$, see figure 4. As a whole, by elongating the side chains, e.g., **1DA-6DA** are showing more negative electrostatic potential on acceptor side as well as entire systems except donor side. The oligocene chain elongation and acceptor groups might make oxidation more difficult and develop the photo-stability [46].

3.3 *Charge transport properties*

The EA and IE are the remarkable characteristics that would provide assistance to comprehend the charge transport barrier. The IE and EA values were obtained with B3LYP/6-31G** level computation studies and exhibited within table 4. Among organic semiconducting substances, the higher EA will give rise to greater electron transport performance, while lower IE is very important to boost up the hole charge transport competency. The computed IE_a/IE_v and EA_a/EA_v of studied compounds are presented within table 4.

The results showed that nitrogen doping in DTP increased the $IE_{a/v}$, i.e., 0.42/0.44 eV while $EA_{a/v}$, i.e., 0.41/0.38 eV for **1** as compared with DTP, respectively. The $IE_{a/v}/EA_{a/v}$ values significantly decreased/increased in push-pull system **1DA**, where EDGs $-N(CH_3)_2$ were substituted at R_1/R_2 while EWDGs $-CF_3$ at R_3/R_4 positions of **1**. Furthermore, it can be observed that by incorporation of anthracene, tetracene and pentacene at both ends lowers $IE_{a/v}$ values as compared to **1DA**. It can be perceived that by elongating the acene cores at both ends considerably enhance the $EA_{a/v}$ than that of **1DA**. The smaller $IE_{a/v}$ while greater $EA_{a/v}$ values are illuminating that hole and electron injection ability in these compounds would be superior than those of DTP and **1**. The lower/higher IE/EA disclosed the fact that these designed derivatives might be good *p*- and *n*-type materials.

The important parameter λ is the quantity that is used for the assessment of substance ability to carry out charge [36,47]. The estimated λ value at B3LYP/6-31G** level for electron λ(e)/hole λ(h) is displayed within table 4. It can be seen that nitrogen doping in DTP increase the λ(h) and λ(e), i.e., 37 and 65 meV, respectively. One can see that anthracene, tetracene and pentacene fusion at both ends help to decrease the λ(h) and λ(e) in designed compounds **4DA-6DA** than those of DTP and **1**. The λ(h) as well as λ(e) were associated with well-known referenced compounds and give an explanation over the charge transport behaviour of newly designed products. The computed λ(e) of **1DA-3DA** are smaller as compared to λ(h), disclosing that these compounds may act as best electron transport candidates. The computed λ(h) of **1**, **4DA** and **5DA** are smaller as compared to λ(e), disclosing that these

compounds may act as best hole transport candidates. The computed λ(h) and λ(h) of **6DA** are alike that is divulging that this compound may act as balanced charge transport hole as well as electron transport candidate. The value of λ(h) of anthracene at B3LYP/6-31G** level is 0.138 [24]. The results given in table 4 showed that the λ(h) of **6DA** is 4 meV smaller than the anthracene, enlightening that this new designed molecule could be comparable hole transport ability as of anthracene. For **6DA**, λ(h) is almost similar to anthracene which demonstrated that this compound might act as a good hole transfer candidate. Additionally, the calculated λ(e) value of commonly used electron transport material *mer*-Alq3 is 0.276 eV [48]. The results showed that values for λ(e) of **4DA-6DA** are 43, 105 and 143 meV lower than the *mer*-Alq3, demonstrating that for these derivatives electron mobility values may be enhanced/comparable with *mer*-Alq3. Thus, it is anticipated that **4DA-6DA** would be efficient materials to be used as *n*-type in semiconductor devices.

4. Conclusions

By donors–acceptors substitution and oligocenes incorporations, electronic and charge transport properties have been successfully tuned. The formation of HOMO charge has been delocalized on donor side while LUMO localized on central electron-deficient ring and/or acceptor side, resulting in ICT from HOMOs to LUMOs. The oligocene chain elongation and acceptor groups might make oxidation more difficult and develop the photo-stability. The smaller $IE_{a/v}$ while greater $EA_{a/v}$ values exposed that hole and electron injection aptitude in **1DA-6DA** would be superior than DTP and **1**. The smaller λ(h) values of **1**, **4DA** and **5DA** than λ(e) are revealing that these derivatives may act as hole transport candidates, while **1DA-3DA** may show better electron transport ability due to smaller λ(e). The λ(h) and λ(e) of **6DA** are alike that is exposing that this compound may act as balanced charge transport for the holes and electrons. The λ(e) of **4DA-6DA** are smaller than the *mer*-Alq3 that is demonstrating that these materials might show enhanced or comparable electron transfer ability as that of reference compound. The lower/higher IE/EA, smaller reorganization energies values disclosed the fact that designed derivatives (**6DA**) might be a good *p*- and *n*-type material.

Acknowledgement

I would like to acknowledge the financial support of the King Khalid University for this research through a grant RCAMS/KKU/006–20 under the Research Center for Advanced Materials Science at King Khalid University, Kingdom of Saudi Arabia.

References

[1] Zhou R, Yang C, Zou W, Abdullah Adil M, Li H, Lv M *et al* 2021 *J. Energy Chem.* **52** 228
[2] Mesta M, Carvelli M, de Vries R J, van Eersel H, van der Holst J J M, Schober M *et al* 2013 *Nat. Mater.* **12** 652
[3] Green M A, Emery K, Hishikawa Y, Warta W and Dunlop E D 2012 *Prog. Photovolt.* **20** 12
[4] Shrestha S 2013 *Prog. Photovolt.* **21** 1429
[5] Krygowski T M, Cyrañski M K, Czarnocki Z, Häfelinger G and Katritzky A R 2000 *Tetrahedron* **56** 1783
[6] Cao J, London G, Dumele O, von Wantoch Rekowski M, Trapp N, Ruhlmann L *et al* 2015 *J. Am. Chem. Soc.* **137** 7178
[7] Mei J, Diao Y, Appleton A L, Fang L and Bao Z 2013 *J. Am. Chem. Soc.* **135** 6724
[8] Bendikov M, Wudl F and Perepichka D F 2004 *Chem. Rev.* **104** 4891
[9] Anthony J E, Facchetti A, Heeney M, Marder S R and Zhan X 2010 *Adv. Mater.* **22** 3876
[10] Eftaiha A F, Sun J-P, Hill I G and Welch G C 2014 *J. Mater. Chem. A* **2** 1201
[11] Wang Y, Fang D, Fu T, Ali M U, Shi Y, He Y *et al* 2020 *Mater. Chem. Front.* https://doi.org/10.1039/d0qm00038h
[12] Irfan A, Imran M, Mumtaz M W, Ullah S, Assiri M A and Al-Sehemi A G 2020 *Optik* https://doi.org/10.1016/j.ijleo.2020.165530
[13] Di Ventra M, Pantelides S T and Lang N D 2000 *Phys. Rev. Lett.* **84** 979
[14] Irfan A, Al-Zeidaneen F K, Ahmed I, Al-Sehemi A G, Assiri M A, Ullah S *et al* 2020 *Bull. Mater. Sci.* **43** 45
[15] Irfan A, Al-Sehemi A G, Assiri M A and Mumtaz M W 2019 *Bull. Mater. Sci.* **42** 145
[16] Irfan A, Al-Sehemi A G and Muhammad S 2014 *Synth. Met.* **190** 27
[17] Zhang J, Wu G, He C, Deng D and Li Y 2011 *J. Mater. Chem.* **21** 3768
[18] Mahmood A and Irfan A 2020 *J. Comput. Electron.* **19** 931
[19] Minemawari H, Yamada T, Matsui H, Tsutsumi J Y, Haas S, Chiba R *et al* 2011 *Nature* **475** 364
[20] Kim D H, Park Y D, Jang Y, Yang H, Kim Y H, Han J I *et al* 2005 *Adv. Funct. Mater.* **15** 77
[21] Wang L, Nan G, Yang X, Peng Q, Li Q and Shuai Z 2010 *Chem. Soc. Rev.* **39** 423
[22] Anthony J E 2008 *Angew. Chem. Int. Ed.* **47** 452
[23] Anthony J E 2006 *Chem. Rev.* **106** 5028
[24] Ifan A, Chaudhry A R and Al-Sehemi A G 2020 *Optik* **208** 164009
[25] Irfan A, Al-Sehemi A G, Assiri M A and Ullah A 2020 *Mater. Sci. Semicond. Process.* **107** 104855
[26] Dufresne S, Hanan G S and Skene W G 2007 *J. Phys. Chem. B* **111** 11407
[27] Sánchez-Carrera R S, Coropceanu V, da Silva Filho D A, Friedlein R, Osikowicz W, Murdey R *et al* 2006 *J. Phys. Chem. B* **110** 18904
[28] Irfan A, Chaudhry A R, Al-Sehemi A G, Assiri M A and Hussain A 2019 *Comput. Mater. Sci.* **170** 109179
[29] Irfan A 2019 *Results Phys.* **13** 102304
[30] Petersson G A, Bennett A, Tensfeldt T G, Al-Laham M A, Shirley W A and Mantzaris J 1988 *J. Chem. Phys.* **89** 2193
[31] Lee C, Yang W and Parr R G 1988 *Phys. Rev. B* **37** 785

[32] Zhang C, Liang W, Chen H, Chen Y, Wei Z and Wu Y 2008 *J. Mol. Struct. (TheoChem)* **862** 98
[33] Greenham N C, Moratti S C, Bradley D D C, Friend R H and Holmes A B 1993 *Nature* **365** 628
[34] Marcus R A and Sutin N 1985 *Biochim. Biophys. Acta—Rev. Bioenerg.* **811** 265
[35] Tsiper E V, Soos Z G, Gao W and Kahn A 2002 *Chem. Phys. Lett.* **360** 47
[36] Brédas J L, Calbert J P, da Silva Filho D A and Cornil J 2002 *Proc. Natl. Acad. Sci.* **99** 5804
[37] Soos Z G, Tsiper E V and Painelli A 2004 *J. Lumin.* **110** 332
[38] Frisch M J, Trucks G W, Schlegel H B, Scuseria G E, Robb M A, Cheeseman J R *et al* 2016 Wallingford, CT: Gaussian, Inc.
[39] Irfan A, Chaudhry A R, Al-Sehemi A G, Sultan Al-Asiri M, Muhammad S and Kalam A 2016 *J. Saudi Chem. Soc.* **20** 336
[40] http://www2.chemistry.msu.edu/faculty/harrison/cem483/work_functions.pdf
[41] Pearson R G 1985 *J. Am. Chem. Soc.* **107** 6801
[42] Vektariene A, Vektaris G and Svoboda J 2009 *ARKIVOC* **2009** 311
[43] Geerlings P, De Proft F and Langenaeker W 2003 *Chem. Rev.* **103** 1793
[44] Politzer P and Truhlar D G (eds) 1981 *Chemical applications of atomic and molecular electrostatic potential* (New York: Plenum Press) p 93
[45] Stewart R F 1979 *Chem. Phys. Lett.* **65** 335
[46] Irfan A, Cui R and Zhang J 2009 *Theor. Chem. Acc.* **122** 275
[47] Marcus R A 1993 *Rev. Mod. Phys.* **65** 599
[48] Irfan A, Cui R, Zhang J and Hao L 2009 *Chem. Phys.* **364** 39